THE JOURNAL OF PHYSICAL CHEMISTRY A

Article

pubs.acs.org/JPCA

Bond-Selective Dissociation of Polyatomic Cations in Mid-Infrared Strong Fields

Suk Kyoung Lee, H. Bernhard Schlegel, and Wen Li*

Department of Chemistry, Wayne State University, 5101 Cass Avenue, Detroit, Michigan 48202, United States

ABSTRACT: Strong field-induced dissociation by intense mid-infrared pulses was investigated in bromofluoroform monocation (CF_3Br^+) and iodobenzene dication ($C_6H_5I^{2+}$) using ab initio molecular dynamics calculations. In both systems, bond-selective dissociation was achieved using appropriate laser polarizations and wavelengths. For CF_3Br^+, energetically disfavored fluorine elimination was strongly enhanced at wavelengths of 7 to 8 μm with polarization along a C−F bond. This is the result of two effects: the deposition of high enough kinetic energy into the molecule by the laser field and the near-resonant excitation of the C−F stretching mode. At shorter and off-resonant wavelengths, bromine elimination becomes significant due to rapid intramolecular vibrational energy redistribution (IVR). For $C_6H_5I^{2+}$, the branching ratios for the dissociation of the *ortho*-, *meta*-, and *para*-hydrogens can be controlled simply by changing the laser polarization. These results show the general applicability of bond selective dissociation of cations by intense mid-infrared laser fields.

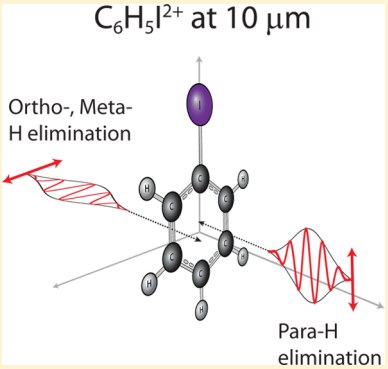

1. INTRODUCTION

Unimolecular reactions are essential chemical processes and have been extensively studied to understand the molecular dynamics in detail and to find ways for controlling specific reactions. Highly energetic molecules can be readily prepared with strong field lasers and readily undergo unimolecular dissociation. Such dissociations often require large nuclear rearrangements with concerted motion corresponding to the reaction coordinate and can occur with or without barriers to form products. Therefore, the deposition of energy into a particular vibrational mode closely coupled to the reaction pathway could drive a molecule along a path toward the desired products.[1] As the most intuitive control method of chemical reactions, bond-selective decomposition has gained much attention over the years. It was hoped that the excitation of a stretching vibrational mode using a tunable laser could achieve bond-selective chemistry. However, it was realized that the initial energy deposited in a particular bond could quickly flow to other vibrational modes on the time scale of the reaction. In particular, infrared multiphoton dissociation (IRMPD) of a polyatomic system is subject to rapid intramolecular vibrational-energy redistribution (IVR)[2,3] and thus generally does not achieve mode selectivity. This is the reason why IRMPD can be described well by statistical methods such as RRKM theory. For example, Bloembergen et al. addressed how IVR can affect the reactivity of a polyatomic system such as CF_3Br when tuning the laser frequency close to the C−F stretching vibration.[4] IVR can lead to an ergodic ensemble within a few picoseconds, resulting in the breaking of the weakest bond, that is, the C−Br bond. Thus, the products of IRMPD with IVR are the same as a thermal reaction. The key for achieving bond-selective chemistry is to suppress IVR. With the advent of femtosecond lasers, defeating IVR becomes possible in time domain. Zewail and coworkers[5] have shown nonstatistical behavior of fragmentation due to ultrafast electronic activation. However, this was accomplished through the limited vibronic states accessible from the Franck−Condon region. Kompa and coworkers[6] reported that direct excitation of the vibration modes coupled to a reaction coordinate by a mid-IR laser pulse drives selective bond breakage on the ultrashort time scale, preventing IVR. A different approach, termed coherent control, has been used to direct chemical reactions using shaped laser pulses and feedback mechanisms.[7−10] Adiabatic passage techniques, such as Raman chirped adiabatic passage (RCAP)[11] and stimulated Raman adiabatic passage (STIRAP),[12] have been studied for controlling the population of excited states and thus chemical reactions. Because the efficiency of population transfer depends on the adiabaticity conditions for chirping, their time scales are limited to approximately picoseconds, hence defeated by IVR. Combining ultrashort IR and UV laser pulses, the control of bond breaking has also been proposed, in which the vibrationally excited wave packets prepared by an IR pulse are transferred to the excited electronic state by a well-timed UV pulse to yield a target product.[13,14] Without exploiting the coherent properties and the ultrafast time resolution of femtosecond laser pulses, vibrational excitation in the ground state has been shown to influence final products resulting from the excitation to higher electronically states, followed by dissociation,[15,16] even though such an excitation scheme does not warrant an ultrashort reaction time.

A new mechanism for bond-specific dissociation was proposed using intense, ultrashort mid-infrared laser pulses in our previous study.[17] This approach differs from previous

Received: April 18, 2013
Revised: August 12, 2013
Published: October 7, 2013

dx.doi.org/10.1021/jp4038649 | *J. Phys. Chem. A* 2013, 117, 11202−11209

experiments with mid-IR lasers mainly through the use of shorter pulses and higher laser intensities – about five orders of magnitude higher than those of conventional IRMPD. Such a high laser intensity leads to significant charge redistribution among constituent atoms and thus alters the molecular potential. Furthermore, because of the long wavelength, atoms could gain a large amount of kinetic energy from the laser field, promoting the chosen reaction on a few hundreds of femtoseconds time scale. The cycle-averaged kinetic energy (i.e., the ponderomotive energy, $U_{pm} = q^2E_{max}^2/(4\mu\omega^2)$, where q is the charge, E_{max} is the maximum electric field strength, μ is the reduced mass, and ω is the laser frequency) scales quadratically with the wavelength, and this becomes significant with mid-IR laser pulses (a few electronvolts for light atoms such as hydrogen). The large kinetic energy forces the dissociation to complete in a very short time and thus prevents IVR from playing a role in the dissociation dynamics. An angular-dependent dissociation yield was observed in formyl chloride cation: the dissociation of a specific bond is dramatically enhanced when the laser polarization is aligned with the bond.[17] This implies that breaking a chosen bond can be accomplished simply by directing the polarization of intense mid-IR pulses parallel to the bond and thus promptly depositing a large amount of energy in the bond.

In this study, we demonstrate how generally applicable this new bond-selective approach is. For two large target systems (CF_3Br^+ and $C_6H_5I^{2+}$), we observed promising bond selectivity, in which energetically disfavored reaction channels dissociate preferentially. We further discuss the benefits and challenges of applying our approach for the bond-selective chemistry.

2. METHOD

Ab initio molecular dynamics (AIMD) was employed to simulate strong-field-induced dissociation. Calculations were carried out with the development version of the Gaussian series of programs[18] using the B3LYP/6-311G(d,p) level of theory. For iodine atom, the Stuttgart effective core potential (SDD ECP) was used for the core electrons. The classical trajectories were computed on the Born–Oppenheimer surface with the recently modified Hessian-based predictor-corrector (HPC) method, which enabled us to study the molecular dynamics of polyatomic systems in strong fields with improved time efficiency.[19] The calculations were carried out on the adiabatic ground electronic state of the two systems (doublet for CF_3Br^+ and triplet for $C_6H_5I^{2+}$). The laser–molecule interaction was modeled using an oscillating electric dipole field. Field-induced transitions between surfaces were not included. Trajectories were integrated with a time step of 0.5 fs, and the Hessian was updated for 10 steps before being recalculated analytically.

The electric field was applied along specific directions in the molecular frames of CF_3Br^+ and $C_6H_5I^{2+}$, as shown in Figure 1A. The maximum field strengths employed in this study are 0.07 and 0.09 au, corresponding the intensities of (1.7 and 2.8) $\times$ 10^{14} W/cm^2, respectively. A five-cycle pulse in the mid-IR range (λ = 6–12 μm) with linear polarization and a Gaussian envelope was used in the simulations; the time evolution of the pulse is shown in Figure 1B. The initial molecular geometries were given zero-point vibrational energy with randomly selected phases and no rotational energy. For each different field orientation and wavelength, a total of 100 trajectories were integrated for up to 0.75 ps. Trajectories were terminated when the distance of atoms in the fragments was over 10 bohrs (5.3 Å).

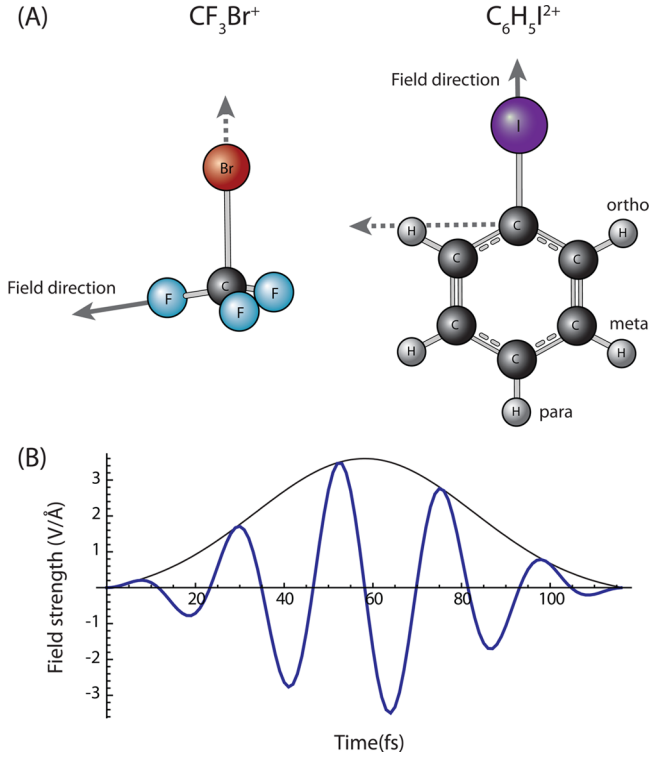

Figure 1. (A) Bromofluoroform monocation (CF_3Br^+) and iodobenzene dication ($C_6H_5I^{2+}$) structures and the field directions defined for classical trajectory simulations. (B) Temporal evolution of the laser electric field with the laser intensity of I_{max} = 1.7 $\times$ 10^{14} W/cm^2 (corresponding field strength is 0.07 au) at 7 μm.

In a strong field with a laser intensity of 10^{14} W/cm^2, neutral molecules are ionized rapidly. Therefore, we chose cations or dications as target systems to avoid the ionization process from complicating the dissociation process. The ionization probabilities for cations or dications are much smaller than those for neutrals due to considerably higher ionization potentials (IPs). Simulations were carried out for the mono cation of bromofluoroform; the triplet dication was chosen for iodobenzene. For the laser pulse selected in this study, we estimated the ionization probability by integrating the ionization rate over the laser pulse. The ionization rate was calculated by a modified ADK (Ammosov–Delone–Krainov) model,[20] in which the ionization rate is associated with the IP. The IPs of the systems (IP = 19.7 and 19.6 eV for CF_3Br^+ and $C_6H_5I^{2+}$, respectively), were computed at the CCSD(T)/6-311+G(2df,2pd) level of theory. The resulting ionization probabilities of both systems are ~3% or less with the maximum field strength of 0.09 au, which can be neglected when compared with the almost 100% dissociation probabilities. However, the estimated ionization probabilities were obtained from IPs calculated at the equilibrium geometries and thus are lower limits. We should account for possible enhanced ionization for deformed geometries during the laser pulse. With the short, intense pulses used in the present study, most of the dissociations occur after the pulse, thereby reducing the possibility of further ionization, as will be discussed later.

3. RESULT

Bromofluoroform Cation (CF_3Br^+). The photodissociation of neutral bromofluoroform is a classical example in which the mode selectivity using IRMPD has failed due to

dx.doi.org/10.1021/jp4038649 | J. Phys. Chem. A 2013, 117, 11202–11209

anharmonic coupling.[4] We show that strong field dissociation by mid-IR laser can achieve this in its cation form. The dissociation energy for bromine elimination channel (0.54 eV, calculated for $CF_3Br^+ \rightarrow CF_3^+ + Br$ at the B3LYP/6-311G(d,p) level of theory) is about one-quarter of the energy for fluorine elimination (2.12 eV), and thus bromine dissociation should dominate according to statistical predictions. The calculation for randomly aligned CF_3Br^+ was first performed in a weak continuous-wave mid-IR laser field ($I_{max} = \sim 2 \times 10^{12}$ W/cm^2 at 7 μm). The results showed that 21 out of 100 trajectories yielded C−F bond dissociation and 79 yielded C−Br bond dissociation. Accounting for the fact that there are three C−F bonds and one C−Br bond, this gives a C−Br to C−F branching ratio of 11:1. This is due to IVR among the coupled vibrational modes (most of the trajectories (93%) are complete within 5 ps). It can be expected that at an even lower intensity the branching ratio for C−Br bond dissociation would be even larger. In contrast, at higher laser intensities and fixed nuclear orientation, the results are dramatically different.

We investigated the normalized yields under different conditions by varying the intensity, the wavelength and the laser polarization along a chosen bond. (See Figure 1A.) In this study, the normalized yield was calculated by dividing the number of trajectories leading to the specific channel by the total number of trajectories. The wavelength dependence of the normalized yields for polarization along a C−F bond is summarized in Figure 2A for two different field strengths. The results clearly show that F elimination is dominant over the range of wavelengths, exhibiting nonstatistical behavior and bond selectivity. The yield of F product has a broad maximum at 7 to 8 μm. The peak becomes somewhat narrower when the maximum field strength is lowered to 0.07 au (and even narrower at 0.06 au (1.3×10^{14} W/cm^2), not shown in Figure 2A). This enhancement of the F yield can be attributed to resonant excitation of the C−F antisymmetric stretching vibrational modes (6.9 μm; all vibrational normal modes are listed in Table 1). With the high laser intensity used in our calculation, it can be expected that the molecular potential is largely suppressed and thus vibration frequencies should be red-shifted, which is consistent with the peak at longer wavelength. Nevertheless, we still observe resonance behavior at such a high intensity. This resonance effect adds an additional control "knob" to our approach using different mid-IR wavelengths. Recently, a similar resonance behavior has been observed in a numerical solution of time-dependent Schrödinger equation (TDSE) of H_2^+ in strong IR fields, in which the dissociation probability increases around the wavelength corresponding to the vibration frequency (also red-shifted).[21] The original idea of IRMPD was that resonant excitation of a specific vibrational mode should correlate with the selected dissociation pathway. The present results indicate that excitation of a particular vibrational mode does play a role in the dynamics of strong-field-induced dissociation, even though the resonance is much broader due to the distortion of the molecular potential by the intense laser field.

The Br elimination occurs generally as a minor channel when the laser polarization is along the C−F bond but is over 20% at 6 μm with the maximum field strength of 0.07 au. At this off-resonance wavelength, Br elimination could be competing with F elimination due to a rapid IVR. It should also be noted that a substantial number (42%) of trajectories do not dissociate within 750 fs. (We refer to these as unfinished trajectories here.) If given enough time, these are likely to result in breaking

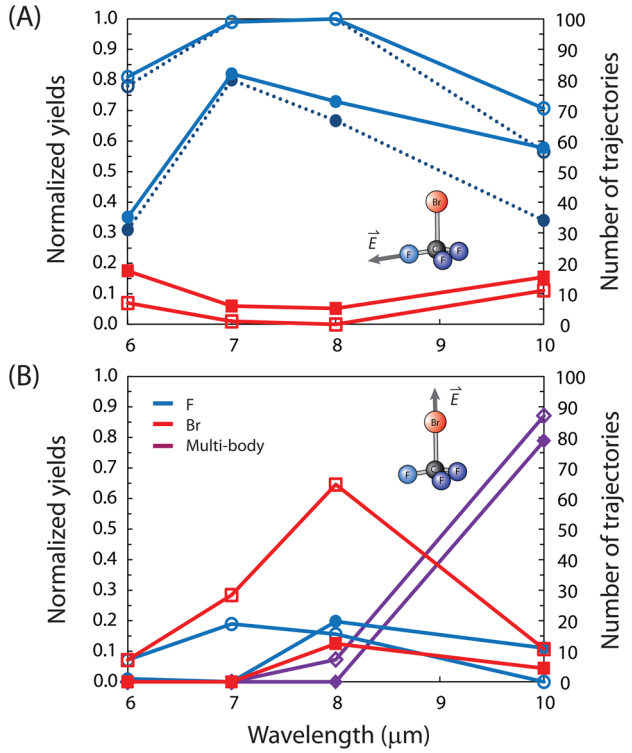

Figure 2. Normalized dissociation yields from bromofluoroform monocations as a function of wavelength: (A) laser polarization along a C−F bond and (B) laser polarization along the C−Br bond. Blue lines represent F eliminations and red lines represent Br eliminations. Closed symbols are for a maximum field strength of 0.07 au; open symbols are for a maximum field strength of 0.09 au. Each simulation consisted of 100 trajectories. The dotted lines in panel A correspond to the normalized yield of the F aligned with the laser field. Purple diamonds in panel B correspond to the normalized yield of multibody dissociation with field strengths 0.07 (closed symbols) and 0.09 au (open symbols).

Table 1. Calculated Vibrational Normal Modes of CF_3Br^+ under Field-Free Condition at the B3LYP/6-311G(d,p) Level of Theory

wavenumber (cm^{-1})	wavelength (μm)	
120	83.3	C−Br stretching
139	72.1	bending
210	47.6	bending
556	18.0	bending
559	17.9	bending
677	14.8	bending
960	10.4	C−F sym. stretching
1449	6.9	C−F antisym. stretching
1452	6.9	C−F antisym. stretching

of the weak C−Br bond after IVR. For example, when we extended the calculation time of a few unfinished trajectories to 10 ps, 70% of them led to Br elimination but none to F elimination, with the rest still not finished within 10 ps. The total energy gained ($\Delta E = \Delta E_{kin} + \Delta E_{pot}$) can indicate whether dissociation can eventually happen. The blue curve in Figure 3 shows that many of the unfinished trajectories have enough energy for Br dissociation at 6 μm and the maximum field strength of 0.07 au. On the basis of this information, we concluded that Br is produced mainly via IVR at 6 μm, especially at lower laser intensities.

dx.doi.org/10.1021/jp4038649 | J. Phys. Chem. A 2013, 117, 11202−11209

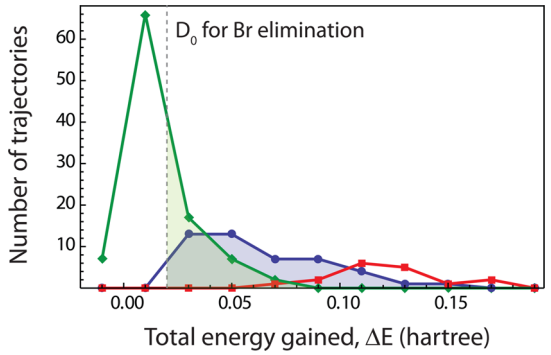

Figure 3. Total energy ($\Delta E = \Delta E_{kin} + \Delta E_{pot}$) gained from the laser field (maximum field strength of 0.07 au and wavelength of 6 μm, 100 trajectories). Red squares and blue circles correspond to Br elimination and unfinished trajectories, respectively, when the polarization is along a C−F bond. Green diamonds correspond to unfinished trajectories when the polarization is along the C−Br bond. The vertical dashed line indicates the threshold dissociation energy of Br elimination.

Figure 2B shows the normalized yields with respect to the driving laser wavelength when the polarization lies along the C−Br bond. The total dissociation probability increases as the wavelength becomes longer and the field strength becomes higher, which is consistent with the fact that the ponderomotive energy is quadratically proportional to the wavelength and linearly proportional to the laser intensity. It is also worth noting that dissociation occurs less when the polarization is along the C−Br bond than when the polarization is along a C−F bond. This is because the ponderomotive potential is inversely proportional to the mass of a constituent atom: the heavier bromine ions gain less kinetic energy from the laser field than the lighter F ions. Figure 3 shows that at 6 μm, with a maximum field strength of 0.07 au and the field aligned with the C−Br bond, most of the unfinished trajectories gain less energy than needed for Br elimination (i.e., these trajectories will not dissociate even with a longer simulation time). For laser polarization along the C−Br bond, we observed reasonable bond selectivity at 8 μm with the higher laser intensity, while no bond selectivity was seen at lower intensities with any of the wavelengths considered. These results indicate that higher field strengths are required to selectively break the C−Br bond. However, the higher field strength can cause significant ionization before dissociation, which suggests that our method may not be efficient for Br dissociation. However, because C−Br bond is the weaker bond, conventional thermal activation or IRMPD should work efficiently.

An interesting result is observed at the longer wavelength (10 μm) for both field directions (along C−Br or C−F bonds): when the polarization is along the C−Br bond, the dominant event is multibody dissociation, in which more than two fragments are produced (see Figure 2B; we considered that bond fission happens when C−F bond lengths reach 3.8 Å (three times the equilibrium distance of C−F) and C−Br bond lengths reach 4.7 Å (two times the equilibrium distance of C−Br), respectively); when the polarization is along a chosen C−F bond (Figure 2A), the dissociation reaches 15−20% for C−F bonds not aligned with the laser field and over 10% for C−Br bond, while at shorter wavelengths the chosen C−F bond exclusively dissociates. However, the major dynamical processes leading to these two observations are quite different and we discuss them as follows.

If the C−Br bond lies along the laser polarization, two effects could contribute multibody dissociation: (1) a higher ponderomotive energy and (2) a near-resonance with the C−F symmetric stretching (10.4 μm). Because of the large ponderomotive energy at 10 μm, even constituent atoms that are not aligned with the field can gain enough energy to dissociate, especially the lighter atoms. Furthermore, polarization along the C−Br bond overlaps with the dipole moment associated with the C−F symmetric stretching mode, enhancing the resonant excitation of this vibrational mode. We further investigate these two aspects by inspecting the time-dependent charge evolutions and angular distribution of product, shown in Figure 4. Indeed, the charge distribution along the C−Br bond changes the most, and fluorine charges fluctuate much more at 10 μm than at 7 μm, implying little or no energy gain from the laser field at the shorter wavelength. If fluorine atoms dissociate

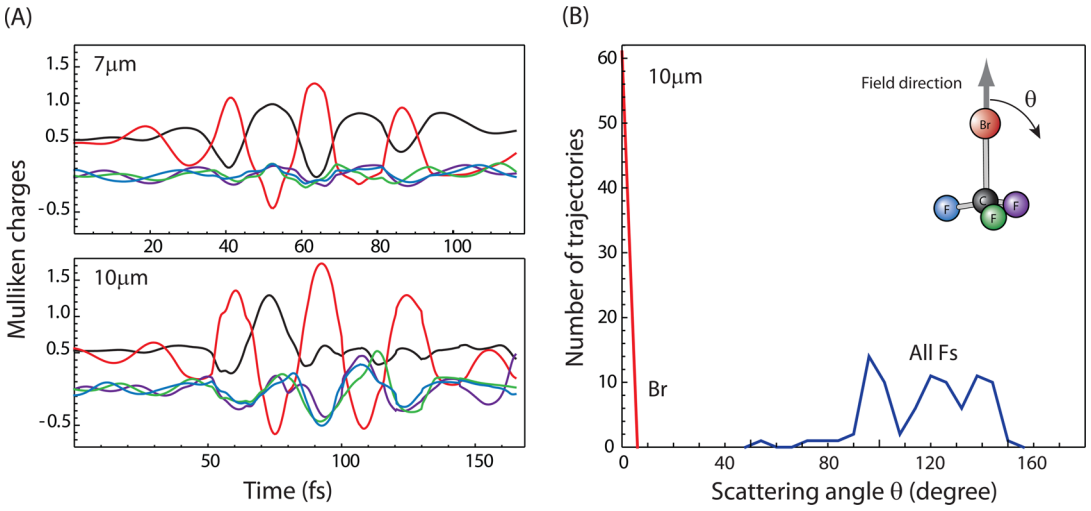

Figure 4. Charge evolution in bromofluoroform ions and the angular distributions of Br and F products when the field is directed along the C−Br bond with the maximum field strength of 0.09 au. (A) Temporal evolution of the Mulliken charge on C (black), Br (red), and F (blue, green, and purple). The top and bottom panels represent charge evolution at 7 and 10 μm, respectively. (B) Angular distributions of recoiled Br (red) and F (blue) atoms at 10 μm (100 trajectories); θ is the angle between the recoil direction and the polarization axis (C−Br bond). The fluorine angular distribution was obtained for all three fluorine atoms.

dx.doi.org/10.1021/jp4038649 | J. Phys. Chem. A 2013, 117, 11202−11209

Table 2. Normalized Yields for Dissociation Channels, Dissociation Probabilities and Average H^+ Dissociation Times of Iodobenzene Dication ($C_6H_5I^{2+}$) for Different Laser Pulse Parameters at a Wavelength of 10 μm

	channel					
polarization	I^+	*ortho*-H^+	*meta*-H^+	*para*-H^+	P_d	avg. time for H^+ dissociation (fs)[c]
Field Strength of 0.09 au						
parallel to C−I[a]	0	0	0	1	1	84
perpendicular to C−I[a]	0	0.49	0.35	0	0.85	117
Field Strength of 0.07 au						
parallel to C−I[a]	0.09	0	0	0.84	0.93	114
parallel to C−I[b]	0.05	0	0.01	0.57	0.63	104

[a]Five-cycle Gaussian pulse with a phase of 0°, 100 trajectories. [b]Four-cycle Gaussian pulse with a phase of 180°, 100 trajectories. [c]Dissociation time is when the distance of atoms in fragments reaches 5.3 Å.

directly by the energy deposited from the laser field, then we should see fluorine atoms scattered along the polarization axis because they preferentially dissociate when they are closely aligned with the laser field. However, fluorine has a broad angular distribution, as seen in Figure 4B, and no fluorine atom is observed within 45° of the laser polarization. By contrast, the angular distribution of bromine atoms is very sharp, which is the character of the direct dissociation. This suggests that a direct dissociation mechanism for C−F dissociation due to a large ponderomotive potential can be ruled out. Additional calculations at 12 μm (not shown) yield 100% Br dissociation and no multibody dissociation. Therefore, we conclude that C−F bond multibody dissociations observed at 10 μm are mainly due to resonant excitation of the symmetric C−F stretch.

When the polarization is along a chosen C−F bond, most of the energy deposited into the system results from the large charge oscillation in the C−F bond aligned with the field. This energy can flow to other vibrational modes via IVR, leading to indirect dissociation of the remaining bonds in addition to the direct dissociation of the chosen C−F bond. This is similar to the results from a 6 μm driving laser with the polarization along a C−F bond. The main difference is the production of F atom not aligned with the field at 10 μm, but such dissociation is absent at 6 μm. This is likely due to a higher ponderomotive potential at a longer wavelength. As previously mentioned, the fluorines not aligned with the laser field could gain energy at this wavelength; bromine would gain significantly less energy because of its heavier mass. Even though the energy gained from the field is not enough to dissociate the C−F bonds directly because they are not in resonance, the energy is mainly localized in C−F bonds and the molecules clearly show a different branching ratio from those at 6 μm. The multibody dissociation that is dominant with the polarization along the C−Br bond was not observed. This is not surprising because the vibrational transition moment (symmetric stretching) is nearly perpendicular to this field direction.

It is important to note that at 8 and 10 μm with the maximum field strength of 0.09 au, some of the fluorine yield dissociates within the last laser cycle. For shorter wavelengths at 0.09 au and for all wavelengths studied at a field strength of 0.07 au, the dissociation of CF_3Br^+ occurs after the laser pulse is off. In our previous study we referred to this as field-free dissociation.[17] Because of the high field strength, a large amount of kinetic energy is quickly deposited into specific vibrational modes during the pulse without significantly changing the nuclear geometry, and this is followed by large amplitude stretching of the bond after the pulse. In this situation, we can safely rule out possible increased ionization due to charge-resonance-enhanced ionization (CREI), which becomes significant only when the bond is substantially elongated. The molecule remains near the equilibrium geometry during the pulse, and as previously mentioned, the ionization probability at this geometry is small compared with dissociation.

Iodobenzene Dication ($C_6H_5I^{2+}$). As we have shown so far, our method depends on the capability of varying the laser polarization in the molecular frame; however, it is not trivial to achieve molecular alignment or orientation in the gas phase, which itself is still an active research topic. However, iodobenzene is one of the few systems in which a very high degree of spatial alignment has been achieved experimentally. Laser-induced alignment of this molecule has been obtained by adiabatic excitation[22] and reported to reach $\langle\cos^2\theta\rangle = 0.97$ with sampled molecules in low-rotational temperature.[23] Hence, this molecule is a good experimental candidate for demonstrating bond-selective dissociation by strong mid-IR fields. In this study, the dication was selected because the monocation has a low IP and can be easily ionized further with the laser intensity used here. The ground electronic state of iodobenzene dication is a triplet state. The dissociation energies are 0.7 eV for I^+ elimination and 4.4 eV for H^+ elimination (averaged over the ortho, meta, and para pathways, computed for $C_6H_5I^{2+}$ at the B3LYP/6-311G(d,p) level of theory).

Compared with CF_3Br^+ and the previous study of $ClCHO^{+17}$, the threshold dissociation energies of the desired channels (selective H^+ elimination) are quite high, and thus we looked into the dynamics at long wavelengths to take advantage of the high ponderomotive energy. The normalized yields calculated at 10 μm are listed in Table 2. With a maximum field strength of 0.09 au and polarization along the C−I bond, *para*-hydrogen elimination occurs exclusively, whereas only *ortho*- and *meta*-hydrogen eliminations take place when the polarization is perpendicular to the C−I bond. Because of the high polarizability of the iodine atom, the field-induced charge oscillation is the strongest when the polarization is along the C−I bond. Furthermore, because hydrogen is the lightest atom, it gains much more kinetic energy from the laser field than iodine atoms, and thus selective dissociation can be achieved. The calculation results show that a high degree of control of the normalized yields of *ortho* and *meta* versus *para* hydrogen dissociation can be achieved by manipulating the laser polarization.

With a maximum field strength of 0.09 au, however, the competition from ionization should be carefully considered. Even though the estimated ionization rate at the equilibrium geometry is low for the selected laser pulses, strong field ionization can be amplified by CREI as bond lengths are stretched. Unlike the case of CF_3Br^+, most of the iodobenzene

dx.doi.org/10.1021/jp4038649 | J. Phys. Chem. A 2013, 117, 11202−11209

dications dissociate during the laser pulse due to the light mass of hydrogen, and thus we cannot completely rule out the possibility of enhanced ionization. However, the laser pulse parameters can be optimized to retain high mode selectivity while reducing ionization, for example, with lower intensities. At the lower field strength of 0.07 au, the yield of H^+ is 84%, while the yield of I^+ is 9% (Table 2). Some of the remaining unfinished trajectories would eventually lead to energetically favored I^+ elimination via IVR. In this case, the averaged dissociation time of H^+ elimination is ∼114 fs, corresponding to the second last laser cycle. Here we choose dissociation time as when the distance of atoms in fragments reaches 5.3 Å (10 bohr). Because the laser intensities in remaining laser cycles are not as high as the peak, charge-resonance-enhanced ionization is less likely. We also varied the number of cycles and the phase of a laser pulse to find optimum conditions. A four-cycle laser pulse with a phase of 180° achieves almost 60% yield, and the fast elongation of the C−H bond happens at the last laser cycle, which has relatively low field strengths. With this shorter pulse, dynamical ionization will be reduced significantly together with hydrogen ion yield. However, hydrogen ion production remains the dominant channel among all reaction pathways.

In addition to optimizing the laser pulse for delayed H^+ dissociation in $C_6H_5I^{2+}$, other aspects of charge-resonance-enhanced ionization should be taken into account. CREI is typically seen in the dissociation of diatomic molecules at wavelengths around 800 nm,[24] and has been also demonstrated in the dissociation of CO_2.[25] A similar mechanism was proposed to explain enhanced ionization in polyatomic hydrocarbon molecules at twice the equilibrium internuclear distance.[26] Because of the much lower photon energy in the mid-infrared range (∼0.12 eV for 10 μm), the critical internuclear distance for initiating CREI is near or in the asymptotic region. At these distances, the C−H bond is already broken regardless of the potential ionization dynamics. A recent study of H_2^+ dissociation by infrared pulses showed that ionization is not a prevailing process (less than one-third of the dissociation probability), even though CREI still exists.[21] Therefore, we can reasonably expect that field-induced dissociation of iodobenzene dication will occur in the mid-IR region without substantial ionization.

Electronic excitation during the laser pulse can also compete with dissociation. In many case, this happens even before significant ionization. Substantial nonresonant excitation from the ground state was found in TD-CIS simulations of butadiene in strong fields of 800 nm laser pulses.[27] In our previous study of $ClCHO^+$, the excitation probability is found to be negligible due to the delayed dissociation and the low energy of the long wavelength photons.[17] The delayed dissociation (field-free dissociation) prevents the excitation rate from increasing because the field is already off when the bonds are significantly elongated and the energy levels are close to each other. Given this rationale, most of the CF_3Br^+ trajectories dissociate without significant excitation, while the $C_6H_5I^{2+}$ trajectories would have to be examined more closely because $C_6H_5I^{2+}$ has some low-lying excited states and most hydrogen ions dissociate within the pulse. The TD-CIS approach was employed with the 6-311G(d,p) basis set to calculate the population of the ground and excited electronic states at the equilibrium geometry. To evaluate the excitation probabilities with elongated C−H bonds, we sampled averaged geometries (e.g., C−H bond length of ∼3 Å) from trajectories that correspond to the second last (or last) laser cycle and carried out TD-CIS calculations with the remainder of the pulse. It turns out that the effects of deformed geometries on the excitation probability are small (or negligible) due to low field strengths in remaining laser cycles. The calculated excitation probability is strongly dependent on the field direction due to a large permanent dipole along the C−I bond. Considerable excitation occurs even at long wavelengths with the laser polarization parallel to the C−I bond, while little or no excitation is seen with the polarization perpendicular to the C−I bond for any of the field strengths employed in the study. For the four-cycle laser pulse with a field strength of 0.07 au, 40% of the population of the ground state is transferred to excited states when the polarization is along the C−I bond. Of the remaining 60% in the ground state, more than half should yield *para*-hydrogen elimination (Table 2). Dissociation will occur on the excited-state surfaces and could yield hydrogen, but this is outside the scope of the present study. Because no excitation is seen when the polarization is perpendicular to the C−I bond, this field orientation could be used to achieve *ortho*- or *meta*-hydrogen ion dissociation without excitation. Substantial H^+ elimination can be achieved for polarization perpendicular to the C−I bond if the higher field strengths are used, for example, 0.09 au. For this case, the degree of excitation is still small ($P_e \approx 11\%$) even after considering the effect of elongated bonds. The average dissociation time is at the second last cycle of the pulse, so the ionization probability should also be small.

4. DISCUSSION

The bond-selective mid-IR dissociation approach presented here exploits both the charge oscillation of molecules in strong laser fields and large ponderomotive potentials afforded by the long wavelength of a mid-IR laser. Significant charge oscillations are present in molecular systems with any driving laser wavelength at high intensity because it is a pure electronic effect due to the distortion of the electron cloud. However, it is the ponderomotive potential that enables the energy transfer from the laser directly to the kinetic energy of the nuclei. With the most widely used 800 nm lasers, while the charge oscillation could be very large, the nuclei cannot follow the quick oscillation of the laser field and the electron density, and thus the kinetic energy gain is indirect and inefficient, as reflected by a small ponderomotive potential. Therefore, it is not surprising from this point of view that 800 nm Ti:sapphire lasers are not efficient in dissociating molecules without invoking ionization or even Coulomb explosion. Only weak perturbation of the nuclear configuration is possible, as demonstrated with impulsive Raman scattering excitation of vibrations. Coherent control exploits both electronic and nuclear degrees of freedom with intense Ti:sapphire lasers.[7,8] While coherent control coupled to shaped laser pulses and genetic algorithm enjoyed great success in recent years, its underlying mechanisms are often complicated due to the intertwined processes of ionization and dissociation.

The concept of ponderomotive potential has been widely used in the strong field physics community for calculating the kinetic energy of ionized electrons and the energy cutoff of high harmonic generation. The ponderomotive potential provides a convenient indicator of how much kinetic energy a constituent atom can gain from a laser field, but it is not an upper bound to the instantaneous kinetic energy gain because it is defined as the cycle-averaged kinetic energy for a free charge. In principle, atoms in a molecule can gain as much as four times the ponderomotive potential during only the first half of a laser

cycle before being slowed down during the second half cycle. As discussed in our previous paper, charge oscillation can allow the constituent atoms to continue accelerating rather than slowing down. The final energy gain, however, depends on the actual value of the charge (generally smaller than unit charge) and the details of dynamics (e.g., the phase of laser fields and whether and when the nuclei rescatter from each other).

Finally, it is worth pointing out the technical advancement of producing intense and ultrashort mid-IR pluses required to implement this new approach has been pursued intensively in the ultrafast laser community for a different reason: using a mid-IR laser to drive high harmonic generation to produce intense attosecond pulses. The approaches being investigated include a free electron laser and optical parametrical chirped pulse amplification (OPCPA).[28,29] A more conventional method to produce ultrashort mid-IR laser pulses is to use an optical parametrical amplifier (OPA) pumped by a Ti:sapphire laser. This technique has been widely used to produce milli-Joule level ultrashort pulses in the mid-IR range.[30] Therefore, the implementation of the current approach can be expected in the near future.

5. CONCLUSIONS

A novel mechanism for achieving the bond-selective dissociation with a strong mid-IR laser pulse has been investigated in large polyatomic molecules (CF_3Br^+ and $C_6H_5I^{2+}$) using ab initio classical trajectory calculations. We observed very large enhancements of energetically disfavored reaction channels for both systems. This was accomplished by choosing the laser polarization to be parallel to the specific bond being cleaved. The wavelength dependence of the F yield in CF_3Br^+ dissociation shows that resonant vibrational excitation does play a role in the dynamics of strong field dissociation. The selective bond dissociation in $C_6H_5I^{2+}$ provides a good candidate for experimental implementation because a nearly perfect alignment of this molecule has been realized experimentally. Favorable branching ratios can be obtained by changing the driving laser polarization: pure *para*-hydrogen elimination occurs when the polarization is along the C–I bond. The rapid development of laser technology in the mid-IR range[28−30] and intensive studies of molecular alignment[31] and orientation[23,32] of polyatomics should enable us to implement bond-selective dissociation experimentally using the proposed method, which is simple and general in controlling photodissociation of cations.

AUTHOR INFORMATION

Corresponding Author

*E-mail: wli@chem.wayne.edu. Tel: 1-313-577-8658

Notes

The authors declare no competing financial interest.

ACKNOWLEDGMENTS

This work was supported by a grant from the National Science Foundation (CHE1212281) and Army Research Office. We thank Wayne State University's computing grid for computer time.

REFERENCES

(1) Crim, F. F. State- and Bond-Selected Unimolecular Reactions. *Science* **1990**, *249*, 1387−1392.

(2) Nesbitt, D. J.; Field, R. W. Vibrational Energy Flow in Highly Excited Molecules: Role of Intramolecular Vibrational Redistribution. *J. Phys. Chem.* **1996**, *100*, 12735−12756.

(3) Schulz, P. A.; Sudbo, A. S.; Krajnovich, D. J.; Kwok, H. S.; Shen, Y. R.; Lee, Y. T. Multi-Photon Dissociation of Polyatomic-Molecules. *Annu. Rev. Phys. Chem.* **1979**, *30*, 379−409.

(4) Bloembergen, N.; Zewail, A. H. Energy Redistribution in Isolated Molecules and the Question of Mode-Selective Laser Chemistry Revisited. New Experiments on the Dynamics of Collisionless Energy Redistribution in Molecules Possibilities for Laser-Selective Chemistry with Subpicosecond Pulses. *J. Phys. Chem.* **1984**, *88*, 5459−5465.

(5) Diau, E. W. G.; Herek, J. L.; Kim, Z. H.; Zewail, A. H. Femtosecond Activation of Reactions and the Concept of Nonergodic Molecules. *Science* **1998**, *279*, 847−851.

(6) Windhorn, L.; Yeston, J. S.; Witte, T.; Fuss, W.; Motzkus, M.; Proch, D.; Kompa, K. L.; Moore, C. B. Getting Ahead of Ivr: A Demonstration of Mid-Infrared Induced Molecular Dissociation on a Sub-Statistical Time Scale. *J. Chem. Phys.* **2003**, *119*, 641−645.

(7) Brumer, P.; Shapiro, M. Coherence Chemistry: Controlling Chemical Reactions with Lasers. *Acc. Chem. Res.* **1989**, *22*, 407−413.

(8) Assion, A.; Baumert, T.; Bergt, M.; Brixner, T.; Kiefer, B.; Seyfried, V.; Strehle, M.; Gerber, G. Control of Chemical Reactions by Feedback-Optimized Phase-Shaped Femtosecond Laser Pulses. *Science* **1998**, *282*, 919−922.

(9) Levis, R. J.; Menkir, G. M.; Rabitz, H. Selective Bond Dissociation and Rearrangement with Optimally Tailored, Strong-Field Laser Pulses. *Science* **2001**, *292*, 709−713.

(10) Nuernberger, P.; Wolpert, D.; Weiss, H.; Gerber, G. Femtosecond Quantum Control of Molecular Bond Formation. *Proc. Natl. Acad. Sci. U. S. A.* **2010**, *107*, 10366−10370.

(11) Chelkowski, S.; Gibson, G. N. Adiabatic Climbing of Vibrational Ladders Using Raman Transitions with a Chirped Pump Laser. *Phys. Rev. A* **1995**, *52*, R3417−R3420.

(12) Bergmann, K.; Theuer, H.; Shore, B. W. Coherent Population Transfer among Quantum States of Atoms and Molecules. *Rev. Mod. Phys.* **1998**, *70*, 1003−1025.

(13) Amstrup, B.; Henriksen, N. E. Control of Hod Photodissociation Dynamics Via Bond-Selective Infrared Multiphoton Excitation and a Femtosecond Ultraviolet-Laser Pulse. *J. Chem. Phys.* **1992**, *97*, 8285−8295.

(14) Elghobashi, N.; Gonzalez, L.; Manz, J. Quantum Model Simulations of Symmetry Breaking and Control of Bond Selective Dissociation of FHF^- Using IR+UV Laser Pulses. *J. Chem. Phys.* **2004**, *120*, 8002−8014.

(15) Hause, M. L.; Yoon, Y. H.; Crim, F. F. Vibrationally Mediated Photodissociation of Ammonia: The Influence of N–H Stretching Vibrations on Passage through Conical Intersections. *J. Chem. Phys.* **2006**, *125*, 174309/1−7.

(16) Crim, F. F. Vibrationally Mediated Photodissociation - Exploring Excited-State Surfaces and Controlling Decomposition Pathways. *Annu. Rev. Phys. Chem.* **1993**, *44*, 397−428.

(17) Lee, S. K.; Suits, A. G.; Schlegel, H. B.; Li, W. A Reaction Accelerator: Mid-Infrared Strong Field Dissociation Yields Mode-Selective Chemistry. *J. Phys. Chem. Lett.* **2012**, *3*, 2541−2547.

(18) Frisch, M. J.; Trucks, G. W.; Schlegel, H. B.; Scuseria, G. E.; Robb, M. A.; Cheeseman, J. R.; Scalmani, G.; Barone, V.; Mennucci, B.; Petersson, G. A.,et al. *Gaussian Development Version Revision H.11*; Gaussian, Inc.: Wallingford, CT, 2010.

(19) Lee, S. K.; Li, W.; Schlegel, H. B. HCO^+ Dissociation in a Strong Laser Field: An Ab Initio Classical Trajectory Study. *Chem. Phys. Lett.* **2012**, *536*, 14−18.

(20) Yudin, G. L.; Ivanov, M. Y. Nonadiabatic Tunnel Ionization: Looking inside a Laser Cycle. *Phys. Rev. A* **2001**, *64*, 013409/1−4.

(21) Picón, A.; Jaroń-Becker, A.; Becker, A. Enhancement of Vibrational Excitation and Dissociation of H_2^+ in Infrared Laser Pulses. *Phys. Rev. Lett.* **2012**, *109*, 163002/1−5.

(22) Kumarappan, V.; Bisgaard, C. Z.; Viftrup, S. S.; Holmegaard, L.; Stapelfeldt, H. Role of Rotational Temperature in Adiabatic Molecular Alignment. *J. Chem. Phys.* **2006**, *125*, 194309/1−7.

(23) Holmegaard, L.; Nielsen, J. H.; Nevo, I.; Stapelfeldt, H.; Filsinger, F.; Kupper, J.; Meijer, G. Laser-Induced Alignment and Orientation of Quantum-State-Selected Large Molecules. *Phys. Rev. Lett.* **2009**, *102*, 023001/1−4.
(24) Zuo, T.; Bandrauk, A. D. Charge-Resonance-Enhanced Ionization of Diatomic Molecular-Ions by Intense Lasers. *Phys. Rev. A* **1995**, *52*, R2511−R2514.
(25) Bocharova, I.; Karimi, R.; Penka, E. F.; Brichta, J.-P.; Lassonde, P.; Fu, X.; Kieffer, J.-C.; Bandrauk, A. D.; Litvinyuk, I.; Sanderson, J.; et al. Charge Resonance Enhanced Ionization of CO_2 Probed by Laser Coulomb Explosion Imaging. *Phys. Rev. Lett.* **2011**, *107*, 063201/1−5.
(26) Lotstedt, E.; Kato, T.; Yamanouchi, K. Efficient Ionization of One-Dimensional Acetylene Investigated by Time-Dependent Hartree-Fock Calculations. *Phys. Rev. A* **2012**, *86*, 023401.
(27) Sonk, J. A.; Caricato, M.; Schlegel, H. B. Td-Ci Simulation of the Electronic Optical Response of Molecules in Intense Fields: Comparison of RPA, CIS, CIS(D), and EOM-CCSD. *J. Phys. Chem. A* **2011**, *115*, 4678−4690.
(28) Ross, I. N.; Collier, J. L.; Matousek, P.; Danson, C. N.; Neely, D.; Allott, R. M.; Pepler, D. A.; Hernandez-Gomez, C.; Osvay, K. Generation of Terawatt Pulses by Use of Optical Parametric Chirped Pulse Amplification. *Appl. Opt.* **2000**, *39*, 2422−2427.
(29) Andriukaitis, G.; Balčiunas, T.; Ališauskas, S.; Pugzlys, A.; Baltuška, A.; Popmintchev, T.; Chen, M.-C.; Murnane, M. M.; Kapteyn, H. C. 90 Gw Peak Power Few-Cycle Mid-Infrared Pulses from an Optical Parametric Amplifier. *Opt. Lett.* **2011**, *36*, 2755−2757.
(30) Popmintchev, T.; Chen, M.-C.; Popmintchev, D.; Arpin, P.; Brown, S.; Ališauskas, S.; Andriukaitis, G.; Balčiunas, T.; Mücke, O. D.; Pugzlys, A.; et al. Bright Coherent Ultrahigh Harmonics in the KeV X-Ray Regime from Mid-Infrared Femtosecond Lasers. *Science* **2012**, *336*, 1287−1291.
(31) Lee, K. F.; Villeneuve, D. M.; Corkum, P. B.; Stolow, A.; Underwood, J. G. Field-Free Three-Dimensional Alignment of Polyatomic Molecules. *Phys. Rev. Lett.* **2006**, *97*, 173001/1−4.
(32) Fleischer, S.; Zhou, Y.; Field, R. W.; Nelson, K. A. Molecular Orientation and Alignment by Intense Single-Cycle THz Pulses. *Phys. Rev. Lett.* **2011**, *107*, 163603/1−5.